Experimental and theoretical study of extremely dilute Sc and Fe impurities in Gd and Tb

W. D. Brewer, S. Hauf, and D. Jones
Fachbereich Physik der Freien Universität Berlin, 14195 Berlin, Germany

S. Frota-Pessôa,* J. Kapoor, Yi Li, A. Metz, and D. Riegel
Hahn-Meitner-Institut Berlin, 14109 Berlin, Germany
(Received 29 November 1994)

We have carried out in-beam time-differential perturbed angular distribution experiments on Fe implanted into single-crystal Gd and Tb hosts, where it is found to occupy both substitutional and interstitial sites. For comparison, the simpler systems Sc in Gd and Tb were also studied. Calculations of the local electronic structure, magnetic moments, and hyperfine fields $B_{\rm hf}$ were performed using the real-space LMTO-ASA method for Fe at both sites in Gd and for Sc in Gd, which implants substitutionally. The results of the experiments and calculations of $B_{\rm hf}$ at 0 K agree well and permit a qualitative explanation of the local magnetism. The calculations show an antiferromagnetic coupling of the local Fe moments to the host moments in Gd which is confirmed by the experiments; it persists to temperatures well above T_C. The temperature dependence of $B_{\rm hf}$ and the damping of the spin-rotation spectra are also discussed.

I. INTRODUCTION

Studies of the local electronic structure and magnetism of impurities in metals have proved fruitful in the past for enhancing our knowledge of magnetic materials. However, experiments have been limited to thermally stable systems (i.e., those with a sufficient solid solubility of the impurities in the given host) and theoretical interpretations usually involved phenomenological models.[1,2] Recently, there have been important new developments in *ab initio* theoretical approaches,[3–5] as well as in experimental techniques,[6,7] which have made the investigation of magnetism under "extreme conditions," e.g., in nonalloying systems, accessible to both measurements and calculations. This broadens the base of the entire field of study, allowing critical tests of theoretical approaches and promising to reveal new physical phenomena.

Among such nonalloying systems are the dilute alloys of transition metals (TM) in rare-earth (R) hosts: the limited solubility of many TM elements makes these alloys thermally unstable[8] and thus difficult or impossible to investigate by conventional means. A number of such alloys have been studied in the past using nuclear techniques, such as Mössbauer effect, perturbed angular correlations, and nuclear orientation,[9,10] which can be applied at very low impurity concentrations. However, the results have often been inconclusive and have not been accompanied by information on the lattice location or the chemical state of the impurities. Samples were in general prepared with the aid of thermal methods or separator implantation followed by thermalization at room temperature or by annealing. For example, the Mössbauer effect measurements on FeR alloys reported in Ref. 9 were carried out with samples made by melting trace amounts of radioactive Co (the parent of the ^{57}Fe Mössbauer isotope) into rare-earth ingots, which might well have resulted in the Co (and Fe) occupying interstitial sites or forming intermetallic compounds. The value of the isomer shift (IS) observed, compared with systematics and theory (see below), rather clearly rules out an interstitial site for Fe in Gd, but the possibility of an intermetallic compound (with an IS similar to that of substitutional Fe in Gd) remains, and could in fact explain the observed vanishing of the hyperfine field near 100 K, which was not detected in the present work.

Here, we report experiments on single Sc and Fe atoms in Gd and Tb monocrystalline hosts using the in-beam time-differential perturbed angular distribution (IBPAD) method following recoil implantation of the impurities.[11] This technique involves creating the impurity atoms to be studied by a nuclear reaction, usually induced by energetic heavy ions, and allowing them to recoil into the desired host material, where the precession of their nuclear moments in the local magnetic field is observed via time-resolved γ-ray spectroscopy. It permits the study of extremely dilute systems, including those which are thermally unstable, since the measuring time is of order of μsec.

We also report calculations of the local electronic structure at Fe and Sc impurities in Gd, including both substitutional and interstitial sites for the Fe impurity. They were carried out by applying the RS (real space)-LMTO-ASA scheme[5,12] to calculate the local electronic structure at Fe and Sc impurities in Gd. In these self-consistent, local density functional calculations, the $4f$ electrons of Gd were treated as a half-filled core state, with all spins aligned. We obtain values for the local magnetic moments and the hyperfine parameters (isomer shifts and hyperfine magnetic fields) of the impurities. The results are in general agreement with the observed hyperfine fields and shed considerable light on the magnetic structure of these systems.

0163-1829/95/51(18)/12595(10)/$06.00

A preliminary account of some parts of this work was given in Ref. 13.

II. PROCEDURES

A. Experimental methods

The IBPAD method has been described in detail in the literature.[7,11] Briefly, the impurity atoms to be investigated are produced by heavy ion reactions, leaving their atomic nuclei in excited, aligned nuclear states and with large recoil energies which allow them to escape from the target foil and implant deeply into the desired host material, positioned behind or beside the target. Following the decay of short-lived electronic and nuclear excitations, the impurities arrive at a relatively long-lived (typically 500 ns), aligned nuclear isomeric state, whose magnetic moment precesses around a local magnetic field $\mathbf{B}_{\rm loc} = \mathbf{B}_{\rm ext} + \mathbf{B}_{\rm int}$, given by the vector sum of an applied field $\mathbf{B}_{\rm ext}$ (perpendicular to the beam axis) and internal magnetic fields $\mathbf{B}_{\rm int}$. Deexcitation γ-rays from the decaying nuclear isomeric state are detected in two directions as a function of time after a beam pulse. The resulting time spectra, which are referred to as spin rotation spectra, are corrected for nuclear decay and background, giving a function which resembles the time development of a damped harmonic oscillator. Figure 1 shows examples for ^{43}Sc in Gd,Tb at different sample temperatures. Analysis of these spectra yields three quantities: an amplitude A, a precession frequency ω, and a damping time τ_D. Each implantation site is represented in the spectrum by a characteristic set of these quantities, with ω equal to twice the local Larmor frequency; it is usual to define a reduced local frequency as $\beta = \omega/\omega_0$, where ω_0 is the corresponding frequency in the applied field alone, and to employ the quantity $\beta - 1$ as a measure of the relative strength of the internal fields, $\beta - 1 = B_{\rm int}/B_{\rm ext}$.

After several lifetimes, a new beam pulse replenishes the supply of decaying nuclear isomers, and this cycle is repeated until the desired statistical accuracy of the spin rotation spectrum has been obtained. The concentration of impurity atoms in the sample at the end of such a measurement is of the order of 10^{13} cm^{-3}, corresponding to a relative atomic concentration of about one ppb. The impurities are thus in fact isolated and do not interact with one another; the probability of their interacting with the defect cascades produced by the implantation is also low, as is confirmed by the results. Within the short measuring times, practically no diffusion of the impurities or defects can occur.

In the present experiments, Fe impurities were produced by the nuclear reaction ^{45}Sc(^{12}C,p2n)^{54}Fe on a Sc foil target and recoiled into polished crystals of Tb or Gd directly behind the target foil. A pulsed beam of ^{12}C ions at 43 MeV from the ISL Cyclotron of the Hahn-Meitner-Institut, Berlin, was used to induce the reaction. Decay γ-rays from the $I^\pi = 10^+$ isomer of ^{54}Fe, with a 360 ns halflife and a nuclear g factor of 0.728, were observed as a function of time following each beam pulse. Scandium ions were produced in a similar way by the reaction ^{12}C(^{36}Ar,αp)^{43}Sc using a pulsed Ar beam at 130 MeV on a natural carbon foil target, yielding the $19/2^-$, 473 ns isomer of ^{43}Sc with a g factor of 0.329. Both of these isomeric states are useful for the determination of magnetic interactions at the impurity sites because of their suitable halflives, high yields, relatively large g-factors, and favorable γ-ray anisotropies. We note that electric quadrupole interactions play no significant role in these studies: the moderate quadrupole moments and

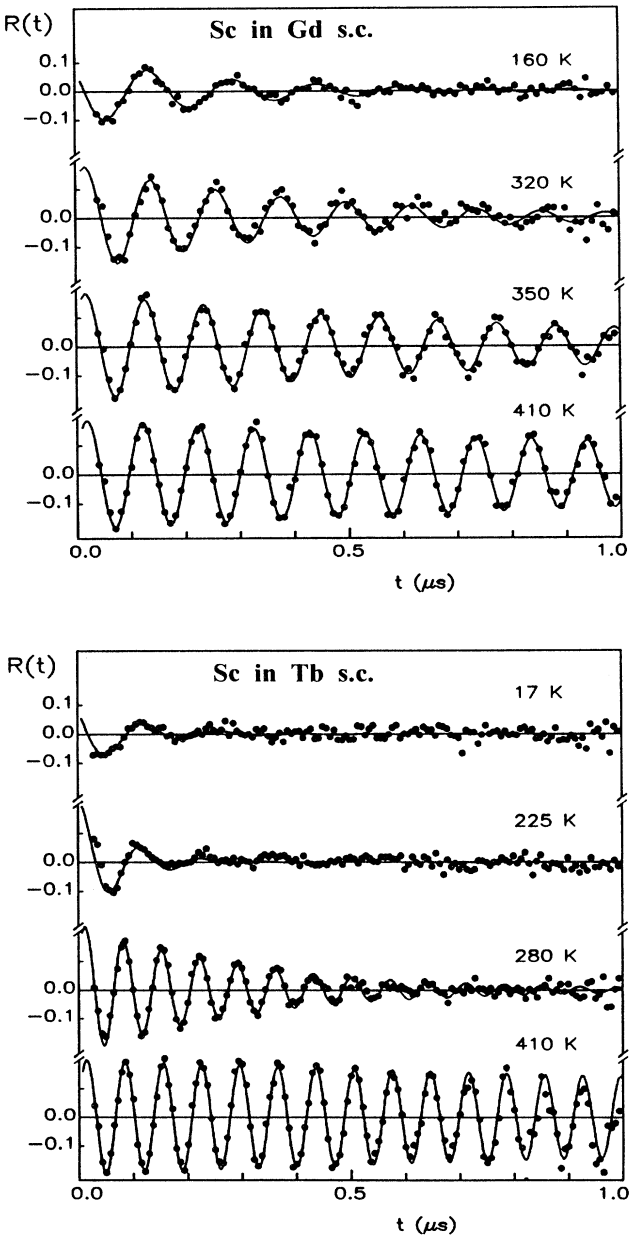

FIG. 1. Spin rotation spectra of ^{43}Sc implanted into Gd (above) and Tb (below). The normalized counting-rate difference from two γ-ray detectors is plotted against time following a beam pulse at the temperatures indicated and at an applied field of $B_{\rm ext} = 2.05$ T. The heavy lines are fits to the theoretical spin-rotation function (damped sine wave).

high spins of the nuclear isomeric states employed make them relatively insensitive to quadrupolar effects. This was verified for Fe in Gd by the absence of any dependence of the observed spectra on the crystal orientation (compare Ref. 14).

The host crystals were made from high-purity Gd and Tb. The Gd crystals were obtained from a commercial supplier and had a nominal purity of 5 N (at. %) with respect to other metals; they were in the form of disks of 5–6 mm diam and about 1 mm thickness, having the hexagonal c axis in the plane of the disks, and were mounted in most cases with the c axis parallel to the applied field. The Tb crystals were obtained from Ames Laboratories and were in the form of slabs of 5 × 5 mm size and about 1 mm thickness. Their preparation and characterization has been described in detail previously.[15] They were mounted with the easy axis of magnetization (the b axis, which was in the plane of the slab) parallel to the applied field. The precision of orientation of the crystal faces and axes was of order 1°–2°. The applied field was in the range 1.95–2.05 T in most cases, and the target-host combination was mounted in a cryostat or a furnace which permitted temperature stabilization and control.

B. Theoretical calculations

The RS-LMTO-ASA scheme is a first-principles, self-consistent procedure based on the well known linear muffin tin orbital formalism in the atomic sphere approximation (LMTO-ASA),[16,17] which uses the recursion method[18] to solve the eigenvalue problem in real space. A detailed description of its application to impurities can be found elsewhere.[12,19] The RS-LMTO-ASA scheme has been used to investigate several metallic systems and the results are in good agreement with those obtained by well established methods. When applied to substitutional impurities, it yields results which agree well with those obtained in the KKR-Green's function formalism.[12] Furthermore, in addition to being an efficient computational method for electronic structure calculations, it has the advantage of allowing the straightforward treatment of sites with low symmetry, such as interstitial sites, and permitting the inclusion of lattice relaxation around the impurity site, as was demonstrated in Ref. 19.

Here, we are interested in calculating hyperfine fields and local magnetic moments at the impurity site. We have carried out a simple nonrelativistic treatment using an exchange correlation term of the form proposed by von Barth and Hedin.[20] In all calculations, a cutoff parameter $L_{\max} = 20$ was taken in the recursion chain; to obtain occupations and higher moments of the local density of states (LDOS), a Beer and Pettifor terminator[21] was used. The $4f$ electrons of Gd were treated as a half-filled core state, with all spins aligned, but the $4f$ levels were not frozen in the atomic configuration; instead, they were recalculated for the appropriate valence configuration at each step of the self-consistent process, as were the $1s - 3s$ inner shells. This approach treats the deep $4f$ shells well, while preventing the appearance of (mostly empty) $4f$ levels near the Fermi level, for which there has been no experimental evidence. These levels, present when the $4f$ electrons of Gd are included as valence electrons in the calculations,[22] are probably due to limitations of the local density functional approximation when applied to highly correlated systems.[23] More details of our calculation procedure can be found in Ref. 24.

Finally, we have used clusters of around 1300 atoms, cut in order to keep the atoms of interest at a maximum distance from the surface, for both substitutional and interstitial impurities. In the case of interstitial Fe, the impurity was placed at the center of the octahedral site and the six first neighbors to the impurity were relaxed outwards by 9% of their distance from the impurity. In the absence of experimental data for relaxation distances, Lennard-Jones pair potentials were used to estimate this quantity. We note that the lattice relaxation cannot be derived directly from the present calculations; however, systematic variation of the assumed degree of relaxation has shown that the derived moments, particularly those of trivalent impurities, are not very sensitive to this quantity. Details of the effects of lattice relaxation will be given in a forthcoming paper. In the present case, the uncertainties in the degree of relaxation are included in the quoted uncertainties in the calculated hyperfine fields.

III. RESULTS AND DISCUSSION

A. Scandium in Gd and Tb

1. Experimental results

We first discuss the simpler case of Sc in Gd and Tb. Since Sc forms solid solutions with both hosts, it is expected to implant preferentially into substitutional sites and give thermally stable alloys; furthermore, Sc should be trivalent in these valence-isoelectronic hosts and thus has formally a closed-shell [Ar] electronic configuration, so that it should not form an intrinsic local moment and its hyperfine field should be due to the host conduction-electron polarization alone. This picture is somewhat oversimplified, as we shall see below.

The spin-rotation spectra for Sc in both hosts exhibit a single component (i.e., one set of the parameters A, ω, and τ_D) at all temperatures (cf. Fig. 1). The amplitude A was found to reach a maximum of about 0.22 just above the Curie temperatures T_C in both hosts; this value is comparable to the largest value observed[25] for ^{43}Sc and indicates that essentially 100% of the implanted ions arrive at similar sites and that no loss of anisotropy (e.g., due to rapid relaxation in defect-associated sites) occurs. In reducing the temperature through T_C, we observe a sudden decrease of the amplitudes by a factor of 2 in both hosts; this effect will be discussed below.

The observed values of β are strongly temperature-dependent, and the internal field, proportional to $\beta - 1$, follows a Curie-Weiss law above T_C:

$$(\beta - 1)^{-1} = \frac{T - \Theta_{\rm loc}}{C_{\rm loc}} . \quad (1)$$

This is shown in Fig. 2 for both Gd and Tb hosts, where similar results are obtained, but with the temperature scale shifted due to the different values of T_C. The figure also contains data for Fe in both observed implantation sites, and for the host magnetizations from Ref. 26. Note that the Curie constant $C_{\rm loc}$ for Sc in Gd and Tb is *negative*, corresponding to a negative slope in Eq. (1) and a negative hyperfine field; the data points have been plotted in Fig. 2 with the signs reversed to allow direct comparison with the magnetization and the Fe data. If the values of the Weiss temperatures are similar (as is seen from Fig. 2 to be the case), taking the ratio of the Curie constants $C_{\rm loc}$ and C_M (from the magnetization data) allows the calculation of the internal field $B_{\rm int}$, using the known magnetization curve of the host and the external field $B_{\rm ext}$. From the relation $B_{\rm int} = B_{\rm hf} + B_{\rm Lorentz} + B_{\rm dipolar} - DM$, magnetic hyperfine fields $B_{\rm hf}$ can then be extracted from the measured $B_{\rm int}$ after corrections for the Lorentz, dipolar, and demagnetizing fields. The hyperfine field can also be derived directly at each temperature by inserting $B_{\rm ext}$ into the definition of $\beta - 1$. At the lowest temperatures, $B_{\rm hf}(0)$ is found to be $-5.22(1)$ T for Sc in Gd and $-3.91(3)$ T in Tb host, using the values of $B_{\rm Lorentz}$ from Ref. 10 and taking $B_{\rm dipolar}$ to be negligible; the quoted errors are purely statistical. These values agree well with those determined previously by nuclear orientation,[10,14] -5.50(65) T and -3.35(40) T for Sc in Gd and Tb, respectively.

At higher temperatures, the hyperfine fields deviate from proportionality to the host lattice magnetization $M(B,T)$; these deviations can be described by a "reduction factor" f, which would be unity for strict proportionality of $B_{\rm hf}$ to $M(B,T)$. Above T_C, f is roughly constant, as can be seen from Figs. 3 and 4. In Fig. 3, the derived values of $B_{\rm hf}$ are plotted against temperature and compared to the magnetization data from Refs. 26 and 27. Figure 4 shows the reduction factor f for Sc in both hosts; the constancy of f above T_C leads to the Curie-Weiss laws, but because f is less than unity, $B_{\rm hf}(0)$ derived from the Curie constants is reduced by a corresponding factor compared to the values determined directly from the low-temperature data and quoted above.

2. *Theoretical calculations for Sc in Gd*

Here we use the RS-LMTO-ASA scheme to obtain the electronic structure around a Sc impurity in Gd. In the

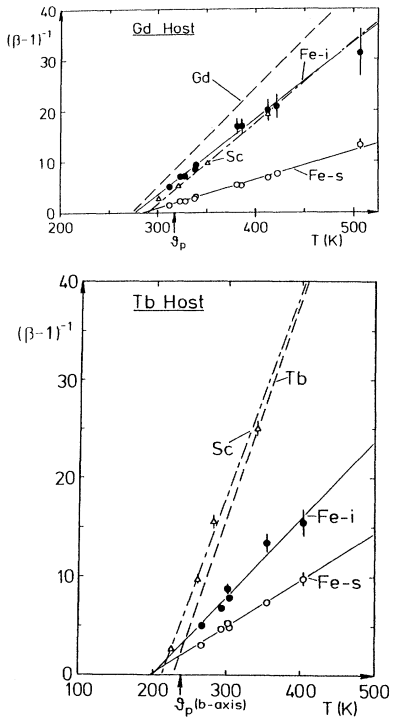

FIG. 2. The Curie-Weiss behavior of the internal fields ($\beta - 1 = B_{\rm int}/B_{\rm ext}$) of Sc (triangles) and Fe (circles: solid = interstitial and open = substitutional sites) impurities in paramagnetic Gd host (above) and in Tb host (below). The slopes of the lines for Sc impurities are in fact negative and have been reversed here for compactness. The dashed lines labeled Gd and Tb refer to the inverse relative host magnetizations, $[M(B,T)/M(\text{sat})]^{-1}$, which also obey Curie-Weiss laws in the applied field $B_{\rm ext} = 2$ T. The arrows at ϑ_p indicate the paramagnetic Weiss temperatures of the hosts.

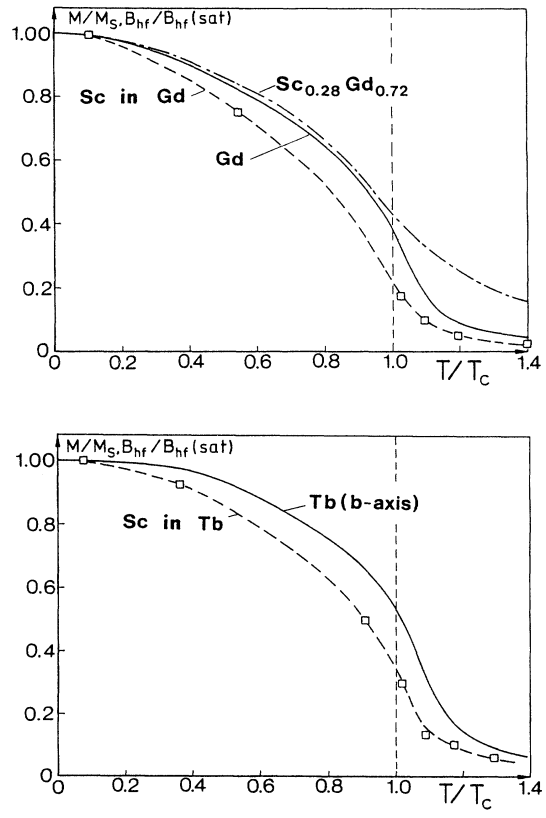

FIG. 3. Reduced magnetizations of Gd and a ScGd alloy (upper plot) and of Tb along the easy axis (lower plot) vs reduced temperature, compared to the reduced hyperfine field $B_{\rm hf}/B_{\rm hf}(\text{sat})$ of ^{43}Sc in the two hosts. The dashed line is a smooth curve connecting the $B_{\rm hf}$ points; the solid and chain curves are from Refs. 26 and 27.

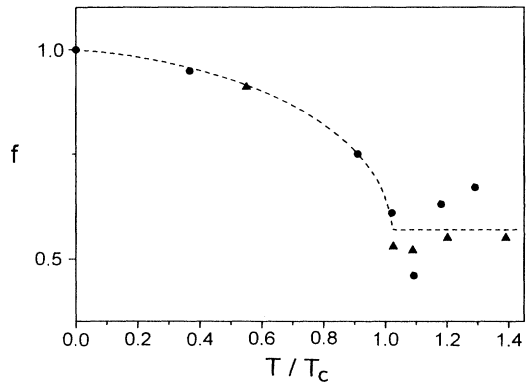

FIG. 4. The reduction factor f, defined as the ratio of the reduced hyperfine field of Sc to the reduced magnetization of the host at the given temperature, vs reduced temperature, indicating deviations from strict proportionality of the hyperfine field to the host magnetization. The circles refer to Gd and the triangles to Tb host; the dashed line is a guide to the eye.

present calculations, the potentials at the Sc impurity and at the 12 Gd atoms in the first neighbor shell were included self-consistently. For the remaining sites in the large 1300-atom cluster, Gd bulk potentials were used. To obtain the Gd bulk potential and the Fermi energy to be used in the impurity calculation, we performed RS-LMTO-ASA calculations for bulk Gd in the hcp structure, using the experimentally observed lattice parameter and c/a ratio. In Fig. 5(a), we show the LDOS of Gd obtained from the real-space calculations. We note that the shape of the LDOS is in good agreement with others given in the literature, which were obtained using the more traditional k-space methods.[22,28] As pointed out above, the $4f$ electrons of Gd were treated here as a half-filled core state with all spins aligned, giving a $7\mu_B$ contribution to the local magnetic moment at the Gd site.

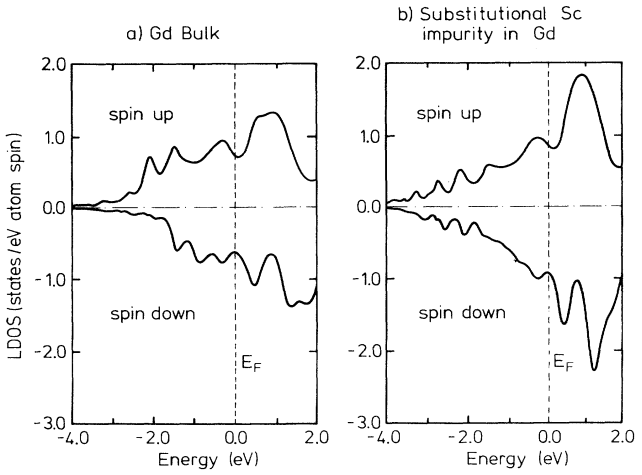

FIG. 5. Local density of states (LDOS) plots for (a) hexagonal Gd and (b) substitutional Sc impurities in Gd obtained by the RS-LMTO-ASA method.

We find that the valence electrons are polarized by the core $4f$ states, resulting in a total magnetic moment of $7.67\mu_B$ per Gd atom, in good agreement with experiment and other calculations.[26,29,22,28]

Figure 5(b) shows the LDOS at the impurity site for substitutional Sc in Gd. The LDOS of spin-up and spin-down states at the impurity are slightly different due to the interaction with the distinct up and down states of the magnetic host; this is a clear example of an induced local impurity moment. This behavior is to be expected, by analogy with the impurity behavior in Y, since the substitutional Sc impurity in Y does not show a local magnetic moment (Y is very similar to Gd in size, number of valence electrons and structure, but since it does not have a polarized core, it is not magnetic). For the Sc impurity in Gd, we find a small induced local magnetic moment of $0.24\mu_B$ aligned parallel to the host moments and arising mainly from p and d valence polarizations. A very small s moment (of order $0.01\mu_B$), antiparallel to the host moment, is also present at the Sc site. This has an interesting consequence for the behavior of the hyperfine fields: we find, as expected for such a small local magnetic moment, a rather small core contribution to the hyperfine field at the site, which is negative and of order of -1 T. Normally, the $4s$ valence contribution would be positive, partially canceling the core contribution. Here, however, the antiparallel alignment of the Sc $4s$ polarization gives rise to a negative valence contribution of around -4 T to the hyperfine field. The resulting value of -5 T for the net hyperfine field at the Sc impurity is in excellent agreement with experiment.

B. Fe in Gd and Tb

1. *Experimental results*

We now turn to the more complex case of Fe implanted into Gd and Tb. The vanishing solubility of Fe-group elements in lanthanide hosts[8] has led to the prediction that they may form stable interstitial alloys in thermal equilibrium. This is supported by the rapid diffusion suggested for Fe in Y host.[30] A recent study of the FeY system[31] combining IBPAD, the in-beam Mössbauer spectroscopy (IBMS) technique, and theoretical calculations established clearly that Fe implants to a considerable extent (about 60%) into interstitial sites in this host, most of the remainder being in substitutional sites. The comparison with the present results is relevant and instructive, owing to the similarity of the Y host to Gd and Tb: Y can be considered to be a nonmagnetic analog of the heavy rare earths.

In Tb and Gd, as in Y, Fe is observed to implant into two lattice sites, as can be clearly seen in Fig. 6, which shows spin rotation spectra for these cases. The two sites, with different amplitudes, precession frequencies, and damping times, give rise to beats in the time spectra; these beats shift as a function of temperature. As in the Y host, the amplitude ratio of the two sites is about 60:40 and is constant over the temperature range observed. By analogy with the Y host, the two signals

can be identified with some confidence as arising from interstitial (majority, site 1) and substitutional (minority, site 2) locations, respectively. In the following, we therefore denote site 1 as the "Fe-i" site, and site 2 as "Fe-s".

The combined amplitudes $A_1 + A_2$ are similar to those observed in Y or Yb hosts, being in the range 0.15–0.17 for Gd and 0.12–0.15 for Tb host (0.16–0.18 in Y, 0.10–0.13 in Yb host[25]). They remain constant up to 900 K; however, as T_C is approached from above, the damping times decrease drastically, and the signals become unobservable for both hosts in the ferromagnetic region, even

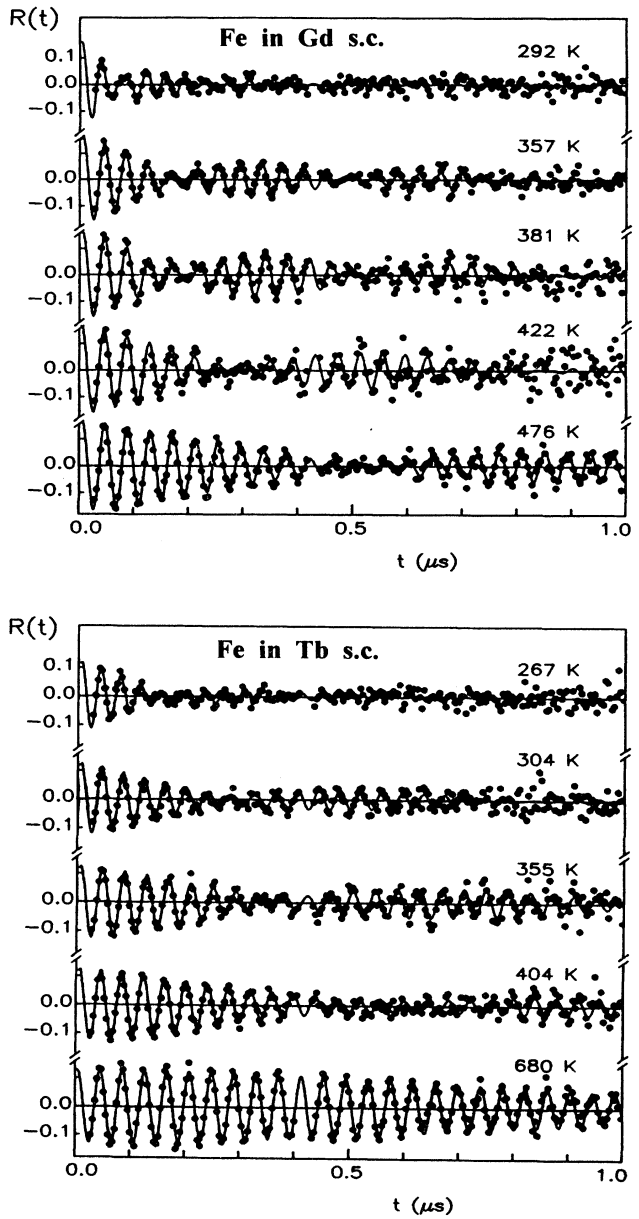

FIG. 6. Spin rotation spectra of ^{54}Fe in Gd host (above) and in Tb host (below) at various temperatures and B_{ext} = 1.95 T; similar to Fig. 1. Note the clearcut beats resulting from the two implantation sites for Fe impurities.

at the lowest temperatures obtainable ($\sim$ 15 K). This is similar to the sudden decrease in A and rapid damping seen for Sc impurities, but leads here to a complete loss of signal within the available sensitivity.

In the paramagnetic regime, the local susceptibilities of both sites again follow Curie-Weiss laws similar to that obeyed by the host magnetization (Fig. 2). The hyperfine fields obtained from the Curie constants or from direct evaluation of β are small and positive on both sites, but distinctly larger for Fe-s. Their low-temperature limiting values $B_{hf}(0)$ can be estimated from comparison of the Curie constants C_{loc} and C_M and the known host magnetization curves, assuming the reduction factor f to be unity; this leads to $B_{hf}(0)$ of about +2 T for the Fe-i site and +6 T for the Fe-s site in Gd host, and +3 T for the Fe-i site, +6 T for the Fe-s site in Tb host. The experimental errors are around 0.1 T in all cases, but are not cited due to the uncertainty of the extrapolation to $T = 0$ assuming $f = 1$. The quoted values can be considered to represent lower limits in view of the possibility that $f \leq 1$. These fields are close to those obtained from Mössbauer effect studies of thermally prepared samples[9,10] without site identification: $B_{hf}(0)$ = +1.85(30) T in Gd and +1.20(20) T in Tb. Again, all of these fields were corrected for the demagnetizing and Lorentz fields of the host. It is tempting to identify the earlier results with interstitial Fe sites in the thermally prepared samples, but this is contradicted by the isomer shift quoted for Fe in Gd in Ref. 9, which agrees well with that calculated here for the Fe *substitutional* site (see below). Reference 9 also reported a drastic decrease in the reduction factor f for Fe in Tb, with f going from near 1 at 50 K to zero at 100 K, which is not indicated by the present results.

The usual negative core-polarization hyperfine fields here appear positive, indicating an antiferromagnetic coupling of the local Fe moments to the host magnetization. This is typical of TM-R alloys with a transition metal from the second half of its d series[32] (R is a heavy rare earth), and has previously been observed (as a ferrimagnetic coupling in concentrated systems), for example in amorphous TM/R compounds[33] and for thin TM/R films.[34] It is reproduced by the *ab initio* calculations for Gd host (see below). A striking feature here is its persistence up to temperatures of several hundred K above the host's ordering temperature in both Gd and Tb, as evidenced by the Curie-Weiss laws for the local susceptibilities (which were verified up to 900 K, where the host magnetization is quite small even in our applied field of 2 T).

2. *Calculations for Fe in Gd and Tb*

We have applied the RS-LMTO-ASA scheme to obtain the electronic structure for both substitutional and interstitial Fe impurities in Gd. In both cases, the potentials at the Fe impurity and 12 Gd neighbors were included self-consistently, while the potentials at the remaining Gd sites in the large 1300-atom cluster were kept at the bulk value. For the substitutional case, these 12

Gd sites included the first shell of neighbors. In the case of interstitial Fe, the impurity was placed at the center of the octahedral site in the hcp structure, and two shells (of six Gd atoms each) around the impurity were included self-consistently. We note that the six neighbors of the first shell around the interstitial Fe impurity were relaxed outwards by 9% of their original distance to the impurity. The bulk potential for Gd and the Fermi energy used in the calculations were obtained as described above (Sec. III A 2).

Since Y and Gd have similar electronic structures, it is interesting to consider what is to be expected for Fe impurities in Gd, based on their behavior in Y host. Several calculations have shown that a substitutional Fe impurity in Y exhibits a large local magnetic moment of about $3\mu_B$, while the interstitial Fe impurity in Y is nonmagnetic.[19] Experimentally, two impurity sites (one magnetic and the other not) are also clearly observed. Based on this evidence, we should expect a strong local magnetic moment for substitutional Fe in Gd and a weak induced local moment (similar to that of Sc) for interstitial Fe in Gd.

In Fig. 7(a), we show the LDOS at the impurity site of substitutional Fe in Gd. We find a local moment of $-3.0\mu_B$, aligned antiferromagnetically relative to the Gd moments. This value is much larger than assumed previously (Refs. 9 and 10), and modifies the curve of $\mu_{\rm loc}$ vs impurity Z for TM impurities in Gd so that it becomes a nearly exact mirror image of that for TM impurities from the $3d$ series in Ni host (compare Refs. 10 and 32). The local moment of Fe in Gd is similar to that of Fe in Y and is clearly not induced by the host magnetism (i.e., by the fact that the spin-up and -down electrons of the host have different densities of states). It is interesting (see Ref. 13) that in the case of substitutional Fe impurities in Gd, a solution (of higher energy) with ferromagnetic alignment and similar magnitude of the local moment can also be found.

In Fig. 7(b), we show the LDOS at the impurity site for interstitial Fe in Gd. We note that, as in the case

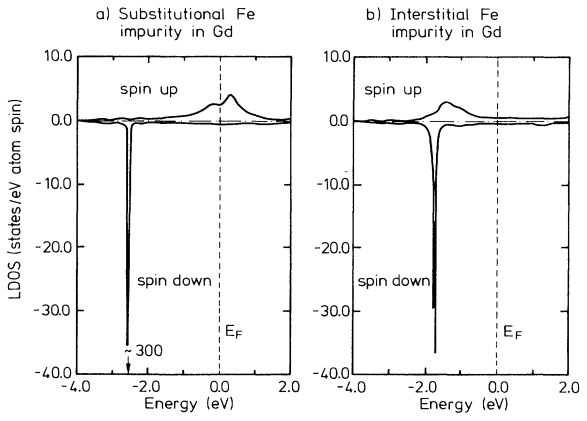

FIG. 7. LDOS plots calculated for Fe impurities in hexagonal Gd at (a) substitutional and (b) interstitial sites. The "spin up" subband is here the minority band due to the antiferromagnetic alignment of the impurity spins.

of interstitial Fe in Y, Sc, Ti, and Zr, the resonant peak which appears in the LDOS is part of a broad d-band which extends far above the Fermi level. Both peaks of the LDOS (for up and down states) are below the Fermi energy. A local magnetic moment of $-1.1\mu_B$, aligned antiferromagnetically relative to the host, is obtained from the calculations. This local moment is not small, and the magnetic behavior seen here is very different from that discussed in the preceding section for a Sc impurity in Gd. But we will give arguments to the effect that the local moment at the interstitial Fe site in Gd is in fact induced, and would not be present if the density of states of the up and down bands of the Gd host were the same. When a moment (or a finite hyperfine field) is observed at an impurity site, the question arises as to whether it is intrinsic or induced in nature. To address this question, we suggest that three criteria can be applied: (i) experimentally, one can place the same impurity into a host with similar electronic and lattice structure, which however does not order magnetically, to see if its moment persists under these conditions; (ii) as a theoretical test, a calculation for the non-spin-polarized impurity can be performed to determine whether the LDOS at the Fermi energy satisfies the Stoner criterion for the appearance of a local moment; and (iii) as a computational check, the host polarization can be artificially reversed with respect to the impurity to see if, as we self-consistently converge the calculation, a new stable solution with reversed polarization will result (if the impurity moment converges to the original configuration found before the reversal of the polarization, we can presume that the moment is induced). In the case of substitutional Fe in Gd, all three criteria point to an intrinsic moment: substitutional Fe in Y is found to be magnetic, the nonpolarized calculations give high values for the LDOS at the impurity site satisfying the Stoner criterion, and two numerically stable solutions (one ferromagnetic and the other antiferromagnetic with respect to the host moment) are found.[13] But, as already pointed out, the interstitial Fe impurity in Y is nonmagnetic,[19] indicating that the local moment of interstitial Fe in Gd is likely to be induced. We therefore performed calculations for a nonpolarized interstitial Fe impurity in Gd. We observe that, as in the case of Y, Sc, Zr, and Ti hosts,[19] the resonant peak in the LDOS appears below the Fermi level and the Stoner criterion is not satisfied. We have also reversed the impurity polarization with respect to that of the host: as the self-consistent solution converges, the impurity moment returns to its original antiferromagnetic configuration, indicating that the interactions with the distinct up and down bands of the host play a major role in determining the moment. All evidence suggests that in the case of interstitial Fe in Gd, what we observe is an unusually large induced local moment, which would not be present if the up and down states of the host had the same LDOS.

We next present results for the hyperfine fields $B_{\rm hf}$ and the isomer shifts (IS) at Fe impurity sites in Gd. Details of the calculational methods can be found in Ref. 24. The present calculations yield for $B_{\rm hf}$ at the substitutional impurity site a core contribution of +30 T and a valence contribution of −26 T, resulting in a net field of

+4 T. At the interstitial site, we find a core contribution of +11 T and a valence contribution of −8 T, resulting in a positive net field of +3 T. We note that in both cases the core contribution is roughly proportional to the local magnetic moment, with a proportionality constant of $10T/\mu_B$. The calculated $B_{\rm hf}$ values are compatible with experiment; but, as explained below, our errors are large, and the theoretical results cannot be used for site identification. The local magnetic moments, isomer shifts, and the core contributions to $B_{\rm hf}$ are rather stable and insensitive to cluster size, the method of terminating the recursion chain and other details of the calculations. Unfortunately, in the case of Fe impurities in Gd, the values of the valence contribution to $B_{\rm hf}$ are not so reliable. Very small variations, of the order of $0.01\mu_B$ in the $4s$-polarization, can produce large changes—of order 5 T—in the resulting valence contribution to the hyperfine field. Errors of this magnitude are thus possible in the numerical results for $B_{\rm hf}$ presented here. We note that this instability with respect to details of the procedure was not seen in the Sc impurity calculations. Finally, we give our calculated IS values: they are +0.25 mm/sec for the substitutional Fe site and −0.30 mm/sec for the interstitial Fe site in Gd. As in the case of Fe in Y, we obtain large positive shifts at the substitutional site and large negative values at the interstitial site. This could be helpful for site identification if Mössbauer experiments are carried out.

C. The damping of the spin-rotation spectra

The observed damping constants τ_D as functions of the sample temperatures are summarized in Fig. 8. For Sc in both hosts as well as for Fe in both implantation sites and both hosts, they increase linearly with temperature in the paramagnetic region. Below T_C, τ_D for Sc impurities is constant, as indicated by the horizontal dashed lines in the figure. The damping rate τ_D^{-1} is given[35] by the sum of the nuclear relaxation rate τ_N^{-1} and the line broadening $\Delta\omega$; the latter is due to a spread in frequencies for nuclei at different locations, causing a rapid dephasing of their precession spectra which results in an effective damping:

$$\frac{1}{\tau_D} = \frac{1}{\tau_N} + \Delta\omega \,. \tag{2}$$

In the Abragam-Pound limit which applies to the present measurements above T_C, the magnetic relaxation rate τ_N^{-1} is field independent, while $\Delta\omega$ is proportional to the applied field (it gives the relative spread in Larmor frequencies); plotting τ_D^{-1} against B thus yields a straight line with its $B = 0$ intercept equal to τ_N^{-1}. This field dependence was measured for both sites of Fe in Gd at a temperature of 358 K; the results are shown in Fig. 9. Equation (2) is seen to be obeyed, with $\Delta\omega$ showing the expected linear dependence on B and having a slope of 1.2 MHz/T at the Fe-s site and 1.6 MHz/T at the Fe-i site. The $B = 0$ intercept is zero within errors in both cases, indicating that the true dynamic relaxation times τ_N are long on the time scale of the present experiments

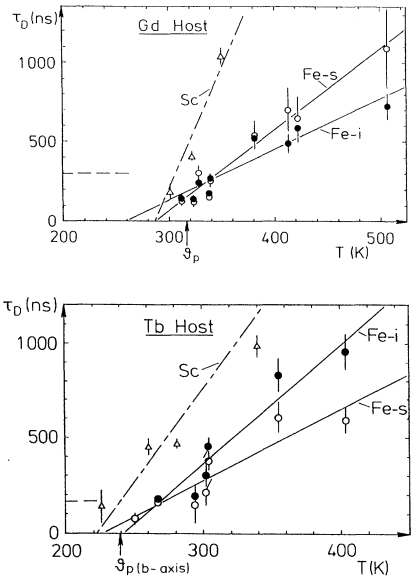

FIG. 8. Damping constants τ_D for Sc and Fe (two sites) in Gd and Tb hosts as indicated. The chain curves are fits of straight lines to the Sc data (only lower temperature points shown), the solid lines are fits to the Fe data, and the horizontal dashed lines indicate the constant values of τ_D observed for Sc in the ferromagnetic regime of the host below T_C.

(i.e., more than several μs). The observed damping is thus dominated by inhomogeneous broadening, at least in the paramagnetic region. Since the field dependence was not determined for Sc, no direct conclusions can be drawn about the origin of the damping in this case, but the very similar temperature dependences found for Sc and Fe in both sites and both hosts suggests that a similar mechanism may be at work here, also. The linear temperature dependence shows similar intercepts on the T axis for each host and site, with values close to the Weiss temperatures observed for the impurity local susceptibilities and for the host magnetizations (Fig. 8). The

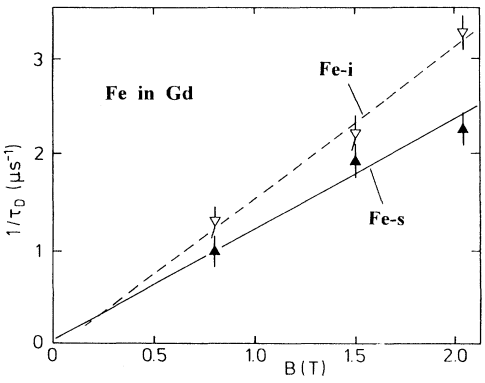

FIG. 9. The dependence on external field B of the damping rates τ_D^{-1} at the two Fe sites is approximately linear and extrapolates to zero at $B = 0$. The data were taken at $T = 358$ K.

temperature dependence of the Sc and Fe damping rates shown in the figure can be explained on a common basis by assuming the inhomogeneous broadening $\Delta\omega$ to be proportional to $B_{\rm int}$. The ratio of the damping constants in the ferromagnetic region is roughly equal to the ratio of the 0 K hyperfine fields in the two hosts, as would be expected if the line broadening were a constant fraction of the average field. Note that our spin-rotation spectra were fitted using an exponential damping for each component, corresponding to the assumption of Lorentzian line shapes; an inhomogeneously broadened line, in contrast, would in all probability have a Gaussian shape. Thus the precise values of τ_D and the amplitudes A quoted here are subject to some uncertainty, which however does not affect our conclusions, since they are not based on a quantitative evaluation of these parameters, but rather on their qualitative behavior.

In passing through T_C, Sc in Gd and Tb exhibits a notable decrease in the amplitudes of the spin-rotation spectra (by about a factor of 2), and a constant value of the damping rate (Figs. 1 and 8), while the spin-rotation of Fe in both hosts becomes unobservable. Most likely, these features are due to a further increase in damping rate τ_D^{-1} for some fraction of the impurities and/or to the presence of a high-frequency component in the spectrum which cannot be resolved by our apparatus (corresponding to net fields above about 20 T). Similar effects were observed in the only other complete study to apply IBPAD to ferromagnetic hosts both above and below T_C, performed by Fahlander *et al.*[36] on ^{19}F implanted into Ni, Fe, and Gd hosts. There, reductions of about 40% in observed amplitudes were seen on passing through T_C, with roughly constant damping rates at lower temperatures. The damping was attributed mainly to a spread $\Delta\omega$ in local frequencies. A direct comparison with the present work is not reasonable in view of the very different physical, chemical, and electronic properties of fluorine as compared to Sc or Fe. The authors of Ref. 36 suggest a spread in dipolar fields, due to varying angles of the crystalline symmetry axes relative to the external field in their polycrystalline samples, as a possible origin of $\Delta\omega$; this explanation is ruled out in the present case owing to the use of single-crystal samples and to the small values of the dipolar field expected at both substitutional and interstitial sites in Gd and Tb.

IV. CONCLUSIONS

We have observed the local magnetic fields and damping rates for dilute Sc and Fe impurities implanted into Gd and Tb single crystals as a function of temperature between 15 K and 900 K using the IBPAD method. For Sc impurities in both hosts, the results support a substitutional implantation site, and give $T = 0$ hyperfine fields in agreement with earlier work which employed thermally prepared samples.[10,14] The net field calculated by the first-principles RS-LMTO-ASA method, $B_{\rm hf}(0) = -5$ T for Sc in Gd, also agrees well with the experimental value, as does its decomposition into a core-polarization contribution from an induced, ferromagnetically aligned local moment of $+0.24\mu_B$ and a negative s-electron contribution of about -4 T (estimated in Ref. 10: $+0.29\mu_B$, -4.4 T). Deviations from strict proportionality of $B_{\rm hf}$ to the host magnetization at higher temperatures are seen in the experiments for both hosts, but they become roughly constant above T_C, so that $\beta - 1$ is fit well there by a Curie-Weiss law similar to those found for the host magnetizations. The observed damping rates and amplitudes of the spin rotation spectra show strong anomalies at T_C and are both constant in the ferromagnetic temperature range of the hosts; the damping rates are roughly in the ratio of the observed $B_{\rm hf}(0)$ values. Above T_C, the damping rates decrease with increasing T and are probably attributable mainly to inhomogeneous broadening.

For Fe impurities, two implantation sites are observed, and they can be identified with some certainty as being interstitial (majority site) and substitutional (minority site), by comparison with the well-studied,[31] analogous alloy Fe in Y. The hyperfine fields $B_{\rm hf}(0)$ at both sites in both hosts are small and positive, and are strongly correlated to the host magnetizations, with similar values in Gd and Tb at the Fe-s sites (about $+6$ T), and somewhat smaller ones at the Fe-i sites ($+2$ – $+3$ T).

This is explained consistently by the first-principles calculations. They indicate a strong, intrinsic local moment of $-3.0\mu_B$ for substitutional Fe in Gd, aligned antiferromagnetically relative to the rare earth moments and thus giving a positive core-polarization contribution to the hyperfine field; it is largely canceled by the strong negative s-electron contribution. This result is qualitatively similar to the previous interpretation,[9,10] but the Fe local moment is much larger than previously assumed. Above T_C, Curie-Weiss laws are obeyed for both sites and both hosts, with intercepts close to those found for the host magnetizations. This is the first clearcut verification of the antiferromagnetic coupling of local *impurity* moments to the rare-earth host and provides a consistent experimental and theoretical description of the TM-R impurity system.

The calculated hyperfine field at the interstitial Fe impurity in Gd is also in reasonable agreement with the present experimental value; however, its decomposition is quite different from that of the substitutional-site field: it results from a surprisingly large, antiferromagnetically aligned but *induced* local moment and a moderate, negative s-electron contribution to $B_{\rm hf}(0)$.

The damping rates at Fe impurities show a similar behavior to those at Sc in the same hosts, but are considerably faster; their applied field dependence in Gd host supports an origin mainly due to inhomogeneous line broadening. Spin-rotation signals were not observable below T_C for either Fe site, and the quoted experimental values of $B_{\rm hf}(0)$ were extrapolated from the paramagnetic region. Finally, the calculated isomer shift for substitutional Fe in Gd is in good agreement with systematics and with the shift at Fe in Gd reported from earlier Mössbauer work,[9] but the sudden decrease of $B_{\rm hf}$ above 100 K reported in Ref. 9 is not confirmed by our experimental results.

ACKNOWLEDGMENTS

We are grateful for the support of Professor F. Mezei and for assistance from Dr. K.-D- Groß and P. Symkowiak, as well as the staff of the ISL Cylclotron. One of us (S.F.-P.) thanks the Hahn-Meitner-Institute, Berlin, for its hospitality. This work was supported in part by the Bundesminister f. Forschung u. Technologie (Grant 03-R12FUB).

---

* On leave from the Instituto de Fisica da Universidade de São Paulo, São Paulo, Brazil.

[1] C. E. Leal and A. Troper, J. Less Common Met. **149**, 377 (1989).

[2] C. E. Leal, L. T. de Menezes, and A. Troper, Solid State Commun. **53**, 35 (1985).

[3] H. Akai, M. Akai, S. Blügel, B. Drittler, H. Ebert, K. Terakura, R. Zeller, and P. H. Dederichs, Progr. Theor. Phys. **Suppl. 101**, 11 (1990).

[4] K. Hummler, M. Liebs, T. Beuerle, and M. Fähnle, Int. J. Mod. Phys. B **7**, 710 (1993).

[5] P. R. Peduto, S. Frota-Pessôa, and M. S. Methfessel, Phys. Rev. B **44**, 13 283 (1991).

[6] E. Dafni, J. W. Noe, M. H. Rafailovich, and G. D. Sprouse, Phys. Lett. **76B**, 51 (1978).

[7] D. Riegel, H. J. Barth, M. Luszik-Bhadra, and G. Netz, in *Valence Instabilities*, edited by P. Wachter and H. Boppart (North-Holland, Amsterdam, 1982), p. 497.

[8] A. R. Miedema and A. K. Niessen, Physica **114B**, 367 (1982).

[9] M. Forker, Hyperfine Interact. **24-26**, 907 (1985); M. Forker, R. Trzcinski, and T. Merzhäuser, *ibid.* **15/16**, 273 (1983).

[10] J. Boysen, J. Grimm, A. Kettschau, W. D. Brewer, and G. V. H. Wilson, Phys. Rev. B **35**, 1500 (1987); W. D. Brewer and E. Wehmeier, *ibid.* **12**, 4608 (1975).

[11] D. Riegel and K.-D. Groß, *Nuclear Physics Applications on Materials Science*, Vol. 144 of *NATO Advanced Study Institute Series E: Applied Physics* (Kluwer Academic, Norwell, MA, 1988), p. 327.

[12] S. Frota-Pessôa, Phys. Rev. B **46**, 14 570 (1992).

[13] W. D. Brewer *et al.*, Proc. ICFE2, 1994 (J. Alloys Compds., in press); H. M. Petrilli and S. Frota-Pessôa, *ibid.*

[14] W. D. Brewer, J. Phys. F **7**, 693 (1977).

[15] W. D. Brewer, P. Roman, M. Böttcher, B. Illerhaus, H. Marshak, K. Freitag, and P. Herzog, Phys. Rev. B **38**, 11 019 (1988).

[16] O. K. Andersen, Phys. Rev. B **12**, 3060 (1975); O. K. Andersen and O. Jepsen, Phys. Rev. Lett. **53**, 2571 (1984).

[17] O. K. Andersen, O. Jepsen, and D. Glötzel, *Highlights of Condensed-Matter Theory*, edited by F. Bassani, F. Funi, and M. P. Tosi (North-Holland, Amsterdam, 1985).

[18] R. Haydock, Solid State Phys. **35**, 216 (1980).

[19] S. Frota-Pessôa, L. M. de Mello, H. M. Petrilli, and A. B. Klautau, Phys. Rev. Lett. **71**, 4206 (1993).

[20] V. von Barth and L. Hedin, J. Phys. C **5**, 1629 (1972).

[21] N. Beer and D. G. Pettifor, in *The Electronic Structure of Complex Systems*, edited by W. Temmermann and P. Phariseau (Plenum Press, New York, 1984).

[22] J. Sticht and J. Kübler, Solid State Commun. **53**, 529 (1985).

[23] D. M. Bylander and L. Kleinman, Phys. Rev. B **50**, 1363 (1994), and references therein.

[24] H. M. Petrilli and S. Frota-Pessôa, Phys. Rev. B **48**, 7148 (1993); also Hyperfine Interact. **78**, 377 (1993).

[25] J. Kapoor, Ph.D. dissertation, Freie Universität Berlin, 1993 (unpublished).

[26] H. E. Nigh, S. Legvold, and F. H. Spedding, Phys. Rev. **132**, 1092 (1963); D. E. Hegland, S. Legvold, and F. H. Spedding, *ibid.* **131**, 158 (1963).

[27] H. E. Nigh, S. Legvold, F. H. Spedding, and B. J. Beaudry, J. Chem. Phys. **41**, 3799 (1964).

[28] B. N. Harmon and A. J. Freeman, Phys. Rev. B **10**, 1979 (1974).

[29] N. Sakai, Y. Tanaka, F. Itoh, H. Sakurai, H. Kawata, and T. Iwazumi, J. Phys. Soc. Jpn. **60**, 1201 (1991).

[30] J. S. Carpenter and W. N. Cathey, Phys. Lett. **A64**, 313 (1977), and references therein.

[31] J. Kapoor, A. Metz, D. Riegel, R. Zeller, K.-D. Groß, P. Schwalbach, M. Hartick, E. Kankeleit, and W. D. Brewer, Europhys. Lett. **24**, 299 (1993).

[32] I. A. Campbell, W. D. Brewer, J. Flouquet, A. Benoit, B. W. Marsden, and N. J. Stone, Solid State Commum. **15**, 711 (1974).

[33] J. M. D. Coey, J. Chappert, J. P. Rebouillat, and T. S. Wang, Phys. Rev. Lett. **36**, 1061 (1976).

[34] B. Scholz, R. A. Brand, W. Keune, U. Kirschbaum, E. F. Wassermann, K. Mibu, and T. Shinjo, J. Magn. Magn. Mater. **93**, 499 (1991).

[35] A. Metz, J. Kapoor, D. Riegel, and W. D. Brewer, Phys. Rev. Lett. **73**, 3161 (1994).

[36] C. Fahlander, K. Johansson, B. Lindgren, and G. Possnert, Hyperfine Interact. **7**, 299 (1979).